

Steven J. BÖING*, Harm J.J. JONKER

Multi-Scale Physics, Delft University of Technology, The Netherlands,

A.Pier SIEBESMA

Royal Netherlands Meteorological Institute (KNMI), De Bilt, The Netherlands & Delft University of Technology

Wojciech W. GRABOWSKI

Mesoscale and Microscale Meteorology, UCAR, Boulder CO, United States

ABSTRACT

Prediction of the transition from shallow to deep cumulus convection remains a challenge in atmospheric modeling. Numerical Weather Prediction and climate models, in which deep convection is parametrized, tend to predict the onset of deep convection too early in the day. However, even Cloud Resolving Models are sensitive to resolution requirements and the representation of microphysics.

In this study we use the Dutch Atmospheric Large Eddy Simulation (DALES) model to conduct detailed simulations of deep convection and investigate to what extent the spatial growth of potential temperature and humidity structures below cloud base influence the transition. When precipitation starts, density currents trigger cloud formation at the edge of areas where rain evaporates. The appearance of such cold pools coincides with a rapid growth of length scales. Previous studies in which the sensitivity of LES simulations to microphysics parameterization was investigated suggest that the evaporation of rain may indeed have a dramatic effect on the development of deep convection (Khairoutdinov and Randall, 2006).

In the present study we try to directly influence the developing spatial structures in the thermodynamical fields by manipulating the contributions in spectral space, i.e. by selectively suppressing/promoting the spectral contribution of particular wavelengths, without modifying the overall (mean) thermodynamical budgets. This enables one to study the effects of organized structures - such as cold pools - separately from the behavior of the model above the cloud layer.

1. INTRODUCTION

Over land in the tropics, it is common that even though there is a large amount of Convective Available Potential Energy (CAPE) at all times and a negligible convective inhibition, shallow cumulus clouds develop in the morning, and a rapid transition to deep convection takes place later in the afternoon. This transition is hard to predict using numerical weather prediction models (Betts and Jakob, 2002; Bechtold et al., 2006; Guichard et al., 2004).

* *Corresponding author address:* Steef Böing, Dept. of Multi-Scale Physics, Delft University of Technology, Delft, The Netherlands (s.j.boing@tudelft.nl - www.msp.tudelft.nl)

A number of recent studies looks into the role of cold pools, which are areas of negatively buoyant air due to rain evaporation. In a simulation without rain evaporation, Khairoutdinov and Randall (2006) found that the rapid growth of deep convection did not occur. Martins et al. (2009) also found a strong correlation between the growth of length scales in deep convection and the occurrence of precipitation. On the other hand, Wu et al. (2009) argue that the transition already occurs before cold pools start to form. A recent observational study by Zhang and Klein (2010) also finds that the inhomogeneity of the surface layer before the onset of precipitation is positively correlated with deep convection.

If cold pools play a role, it can be questioned if they are important because they modify the thermodynamic fields in the subcloud layer (Tompkins, 2001) or if their main effect is to provide additional kinetic energy to lift the parcels (e.g. Rio et al., 2009).

An alternative explanation for the transition is that parcels which reach higher levels can maintain their positive buoyancy (Wu et al., 2009). The relative positive buoyancy of shallow clouds is quite small. In deep convective regimes, an undiluted parcel rising from cloud base becomes strongly buoyant at higher levels in the mid-troposphere. Moreover, gradual moistening at the top of the cloud layer (Derbyshire et al., 2006) and the lateral growth of clouds may reduce entrainment. These effects may explain a rapid change in cloud buoyancy.

We study the processes that play a role in the transition to deep convection using Large Eddy Simulation. In order to get a better grasp of the role of the subcloud layer in the transition, we manipulate the structure of the thermodynamic fields in the subcloud layer in the model.

2. METHOD AND CASE**2.1 Large Eddy Simulation Model**

We use the Dutch Atmospheric Large Eddy Simulation (DALES) model to investigate the transition. An earlier version of DALES is described by Heus et al. (2010). The model uses a prognostic SFS turbulent kinetic energy equation, and works with total water (q_t) and liquid water potential temperature (θ_l) as its thermodynamic variables. In order to make the model suitable for the simulation of deep convection, the following modifications were made: - Rather than the Boussinesq approximations, the anelastic approximations (Lipps and Hermler, 1982) are used.

The pressure gradient is expanded with respect to a mean hydrostatic state (cf. Smolarkiewicz et al., 2001)

- A one-moment ice microphysics scheme has been implemented. The approach taken closely follows Grabowski (1998). The latent heat of melting and freezing is not taken into account in the thermodynamic equation, which implies that the equivalent potential temperature is approximately conserved. A diagnostic graupel class is added to the original scheme (as in Khairoutdinov and Randall, 2006). Coefficients for graupel are taken from Tomita (2008), as this scheme is similar to that of Grabowski (1998). The microphysics scheme does not explicitly account for the interactions between precipitation classes, and rain evaporation may be overestimated due to the fact that we are using a one-moment scheme (Lang et al., 2007; Grabowski and Morrison, 2010). Current work, however, focuses on the identification of mechanisms behind deep convective growth, rather than quantitative accuracy.
- Saturation pressure is calculated with respect to a mixture of cloud water and cloud ice.
- Hydrometeor loading is taken into account in the momentum equation.

2.2 Case description

The case we are investigating is based on the February 23 observations of the TRMM-LBA campaign (Silva Dias et al., 2002). A CRM and single column intercomparison study based on this campaign is described in Grabowski et al. (2006). The simulation starts with initial profiles which correspond to an early morning sounding. Khairoutdinov and Randall (2006) performed high resolution simulations of this case, focusing on the role of entrainment. Lang et al. (2007) investigated the sensitivity of simulations of this case to a number of microphysical processes, in particular autoconversion and accretion.

In this work, we follow the approach of Wu et al. (2009), who simplified the case. The initial potential temperature, pressure and relative humidity profiles are smoothed, radiative forcing is ignored and surface fluxes are taken constant in time and space. This allows us to focus on the intrinsic properties of the transition. In contrast to Wu et al. (2009), we are running fully 3-dimensional simulations.

2.3 LES Setup

A relatively small 51.2×51.2 km domain is used. The horizontal grid spacing is 200 meters, which is rather coarse for the shallow cumulus phase. Vertical grid spacing increases exponentially from 40 meters at the surface to 195 meter at 25 km, the top of the domain. The model is started with small (0.2 K) potential temperature perturbations. The simulation is continued for 8 hours, 2 hours longer than the original case. This enables us to see how much the onset of deep convection is delayed in simulations where the subcloud dynamics are manipulated. Statistics are sampled every minute, 10 minute averages are presented here.

2.4 Subcloud layer modifications in LES

In order to obtain a better understanding of the processes at work, the dynamics of the Large Eddy Simulation are manipulated in some runs. The LES thus serves as a virtual laboratory to investigate cloud behavior.

We will focus on simulations where the thermodynamic fields are modified directly. In order to see if the spatial organization in the subcloud layer is important, we add a forcing that suppresses large scale organisation in the thermodynamic fields:

$$\frac{\partial}{\partial t} \theta_t = \dots + F_{\theta_t}, \quad (1a)$$

$$\frac{\partial}{\partial t} q_t = \dots + F_{q_t}. \quad (1b)$$

where the Fourier transform of the additional forcing F_ϕ with $\phi = \{\theta_t, q_t\}$ is given by

$$\hat{F}_\phi(k_x, k_y, z) = -\frac{1}{\tau(|\vec{k}|, z)} \hat{\phi}(k_x, k_y, z) \quad (2)$$

Here, hats denote the horizontal Fourier transforms of a thermodynamic variable and τ a time scale. The filtering procedure leaves the horizontal average of the thermodynamic fields intact, and retains the structure of small-scale perturbations, whereas it dampens out large scale fluctuations from the field. The time scale depends both on height and on the wave number:

$$\tau = \frac{\tau_0}{f_1(|\vec{k}|) f_2(z)} \quad (3)$$

where

$$f_1(|\vec{k}|) = \frac{1}{2} - \frac{1}{2} \tanh\left(\frac{k - k_{2BL}}{k_{smooth}}\right) \quad (4)$$

$$f_2(z) = \frac{1}{2} - \frac{1}{2} \tanh\left(\frac{z - z_{BL}}{z_{smooth}}\right) \quad (5)$$

Here, $k_{2BL} = \pi/z_{BL}$ is the wave number corresponding to a mode with wavelength twice the boundary layer height and k_{smooth} and z_{smooth} determine the sharpness of the filter. The results presented here use a τ_0 of 30 seconds, $k_{smooth} = 0.1k_{2BL}$ and $z_{smooth} = 0.2z_{BL}$.

In a few simulations, the microphysics parameterization is also modified. Khairoutdinov and Randall (2006) explored the same case without rain evaporation. They found that this greatly reduced deep convection, and argued the reduction was due to the absence of cold pools. Completely ignoring rain evaporation, however, also reduces the amount of water vapor present in the subcloud layer as compared to simulations with evaporation.

An alternative is to not let the rain evaporation act on the local thermodynamic fields, but rather use the horizontal mean evaporation which is diagnosed in the microphysics model to generate θ_t and q_t -tendencies at every point. In this way, the rain evaporation is prevented from introducing additional scales in the subcloud layer,

but evaporation still acts on the mean fields. Total rain evaporation may in fact be higher as compared to the case with 'normal' evaporation, as the positive total water tendency in the subcloud layer below a precipitating cloud constitutes a negative feedback on evaporation.

3. RESULTS AND DISCUSSION

3.1 *Transitional growth of cumulus congestus*

We first simulate a reference case where no forcings are added to the subcloud layer. Figures 1 and 2 show the development of horizontal mean cloud condensate (including ice) and precipitation (including snow and graupel) over time. They are found to be in good agreement with figure 4 in Wu et al. (2009, the M85 case) and figure 15 in Khairoutdinov and Randall (2006), although the transition is somewhat slower in our model as compared to Wu et al. (note that 8 hours are shown instead of 6). This is possibly due to the fact that convective updrafts are less likely to entrain enough to terminate in 2-dimensional simulations (Petch et al., 2008; Grabowski et al., 2006).

Figures 3 and 4 show the development of cloud condensate path and precipitation path over time. When precipitation becomes strong after 5 hours, this coincides with a deviation from linear increase of the cloud center of mass. The cloud condensate path is within the range of the intermodel comparison in Grabowski et al. (2006). Wu et al. (2009) found that at the time of transition, the 'average cloud' (average of all cloudy points) became buoyant with respect to its environment. Figure 5 shows the mean horizontal buoyancy (expressed as a difference in virtual potential temperature), sampled on cloudy points. The rapid change of center of mass is indeed accompanied by the occurrence of a positive average cloud buoyancy. Figure 6 shows the sampled vertical velocity, which is well correlated to the buoyancy.

3.2 *Behavior of the subcloud layer*

Figure 7 displays a horizontal slice of subcloud buoyancy at 100 meters after 3, 5 and 7 hours. There is a pronounced presence of cold pools after 5 hours. After 7 hours, individual cold pools take up a large part of the domain. As our domain is periodic, cold pools may start to interact with themselves, and a larger domain size would be needed to continue the simulation.

Figure 8 shows the corresponding vertical velocity field. Strong downdrafts occur in relatively small areas in the center of the cold pool, whereas updrafts occur along lines at the edge of the cold pool. Figure 9 shows the local rain water path. Precipitation only occurs in the center of cold pools, the surrounding negatively buoyant air is a result of density currents generated by evaporation at higher levels.

3.3 *LES experiments with modified subcloud dynamics*

Figure 10 shows the development of the cloud condensate path and the precipitating water path in the case with

a direct forcing to prevent large scales. The change in location of the center of mass is shown in figure 11. Filtering delays the onset of precipitation, but once precipitation occurs, there is a very rapid transition to deep convection. Figures 18.A and 18.B show the buoyancy field at 100 meters after 5 and 7 hours respectively. The strong cold pools from the reference case have disappeared. After 5 hours, there is almost no large scale organisation in the subcloud layer. After 7 hours, however, the convection is organized in concentric rings, which resemble interference patterns. These structures are not filtered out in Fourier space. Apparently, the filtering procedure feeds back on the small scale dynamics.

Comparison with vertical slices of buoyancy and liquid water field (not shown) indicates that in the filtered simulations, deep convection occurs above these rings. The convection behaves in a different way from cold pools. In the reference case, the location of cold pools changes over time. On the other hand, the structures are stationary when the forcing is implemented, as seen in the buoyancy fields after 5 and 7 hours.

Other ways to manipulate the subcloud layer are also considered. When the evaporation acts on the mean thermodynamic fields, both cloud condensate path and precipitation path increase gradually throughout the simulation and the cloud center of mass also loses its rapid pickup (figures 12 and 13). The subcloud layer is still organized on scales comparable to the boundary layer height after 7 hours, as seen in figure 18.C, i.e. lacking large scale organisation.

The cloud clusters in the filtered simulations develop in areas where there is locally very strong evaporation. In simulations where the strength of precipitation is reduced by leaving out accretion, the cold pools become weaker. The effect of filtering also becomes much more pronounced. The cloud condensate and precipitation paths at the end of the simulation are now lower in the case with additional forcing (figures 14,15,16 and 17). The reference case without accretion shows cold pools after 7 hours, whereas the forced case is still dominated by boundary layer-size dynamics (figures 18.D and E).

3.4 *Does entrainment change in the transition?*

The results from the filtering experiments suggest that structures in the subcloud layer are important for deep convection. One possibility is that these structures influence the entrainment of clouds at a higher level. Grabowski et al. (2006), for example, found that mean cloud width gradually increased during the transition. We looked at the profiles of θ_e (figure 20 and 19), using both a simple conditional sampling on in-cloud and environmental values and sampling on the basis of distance to the cloud. The difference between cloud and environment is very pronounced. The bulk plume fractional entrainment for θ_e is defined here as

$$\epsilon_{plume} = \frac{\partial_z \theta_{e,clد}}{(\theta_{e,env} - \theta_{e,clد})} \quad (6)$$

As figure 21 shows, the bulk plume entrainment of θ_e drops to a value close to zero, where the numerator of the entrainment becomes very low. Even though the bulk plume approach may have its limitations, the persistence of the difference between in-cloud and environmental values of θ_e up to higher levels is striking.

4. CONCLUSIONS

The Dutch Atmospheric Large Eddy Simulation model is used to simulate the transition from shallow to deep convection over land. The timing of the transition is in good agreement with previous studies, and can be influenced by manipulating the subcloud layer thermodynamic fields or the effect of evaporation. It thus appears that the organization of the subcloud layer plays a crucial role. Future work will look into changing the filtering procedure for large scale perturbations, in order to prevent the concentric rings from appearing. It will also look further into the relation between organization in the subcloud layer and entrainment. In order to obtain a more realistic representation of the surface layer dynamics, the effect of interactive surface fluxes will also be investigated.

ACKNOWLEDGMENTS

This work was sponsored by the National Computing Facilities Foundation (NCF) for the use of supercomputer facilities, with financial support of NWO. The authors wish to thank Dr. Chien-Ming Wu for his help in constructing the initial profiles for this case.

REFERENCES

- Bechtold, P., J.-P. Chaboureaud, A. Beljaars, A. K. Betts, M. Köhler, M. Miller, and J.-L. Redelsperger, 2006: The simulation of the diurnal cycle of convective precipitation over land in a global model. *Quart. J. Roy. Meteorol. Soc.*, **130**, 3119–3137.
- Betts, A. and C. Jakob, 2002: Evaluation of the diurnal cycle of precipitation, surface thermodynamics, and surface fluxes in the ecmwf model using lba data. *J. Geophys. Res.*, **107**, 8045.
- Derbyshire, S., I. Beau, P. Bechtold, J.-Y. Grandpeix, J.-M. Piriou, J.-L. Redelsperger, and P. Soares, 2006: Sensitivity of moist convection to environmental humidity. *Quart. J. Roy. Meteorol. Soc.*, **130**, 3055–3079.
- Grabowski, W., 1998: Toward cloud resolving modeling of large-scale tropical circulations: A simple cloud microphysics parameterization. *J. Atmos. Sci.*, **55**, 3283–3298.
- Grabowski, W. and H. Morrison, 2010: Indirect impact of atmospheric aerosols in idealized simulations of convective-radiative quasi-equilibrium. double-moment microphysics. *13th AMS Conference on Cloud Physics*.
- Grabowski, W., et al., 2006: Daytime convective development over land: A model intercomparison based on LBA observations. *Quart. J. Roy. Meteorol. Soc.*, **317-344**, 317–344.
- Guichard, F., et al., 2004: Modelling the diurnal cycle of deep precipitating convection over land with cloud-resolving models and single-column models. *Quart. J. Roy. Meteorol. Soc.*, **131**, 3139–3172.
- Heus, T., et al., 2010: Formulation of and numerical studies with the dutch atmospheric large-eddy simulation (DALES). *Geosci. Model Dev. Discuss.*, **3**, 99–180.
- Khairoutdinov, M. and D. Randall, 2006: High-resolution simulation of shallow-to-deep convection transition over land. *J. Atmos. Sci.*, **63**, 3421–3436.
- Lang, S., W.-K. Tao, R. Cifelli, W. Olson, J. Halverson, S. Rutledge, and J. Simpson, 2007: Improving simulations of convective systems from TRMM LBA: Easterly and westerly regimes. *J. Atmos. Sci.*, **64**, 1141–1164.
- Lipps, F. and R. Hermler, 1982: A scale analysis of deep moist convection and some related numerical calculations. *J. Atmos. Sci.*, **39**, 2192–2210.
- Martins, J., P. Miranda, P. Soares, and J. Teixeira, 2009: Length scale analysis of the transition from shallow to deep convection. *CFMIP/GCSS Boundary Layer WG Workshop on evaluation and understanding of cloud processes in GCMs*.
- Petch, J., P. Blossey, and C. Bretherton, 2008: Differences in the lower troposphere in two- and three-dimensional cloud-resolving model simulations of deep convection. *Quart. J. Roy. Meteorol. Soc.*, **134**, 1941–1946.
- Rio, C., F. Hourdin, J. Grandpeix, and J. Lafore, 2009: Shifting the diurnal cycle of parameterized deep convection over land. *Geophys. Res. Lett.*, **36**, L078009.
- Silva Dias, M. et al., 2002: Cloud and rain processes in a biosphere atmosphere interaction context in the amazon region. *J. Geophys. Res.*, **107**, 8072.
- Smolarkiewicz, P., L. Margolin, and A. Wyszogrodzki, 2001: A class of nonhydrostatic global models. *J. Atmos. Sci.*, **58**, 349–364.
- Tomita, H., 2008: New microphysical schemes with five and six categories by diagnostic generation of cloud ice. *J. Met. Soc. Japan.*, **86A**, 121–142.
- Tompkins, A., 2001: Organization of tropical convection in low vertical wind shears: The role of cold pools. *J. Atmos. Sci.*, **58**, 1650–1672.
- Wu, C.-M., B. Stevens, and A. Arakawa, 2009: What controls the transition from shallow to deep convection? *J. Atmos. Sci.*, **66**, 1793–1806.
- Zhang, Y. and S. Klein, 2010: Mechanisms affecting the transition from shallow to deep convection over land: Inferences from observations of the diurnal cycle collected at the ARM southern great plains site. *J. Atmos. Sci.*, accepted.

5. FIGURES

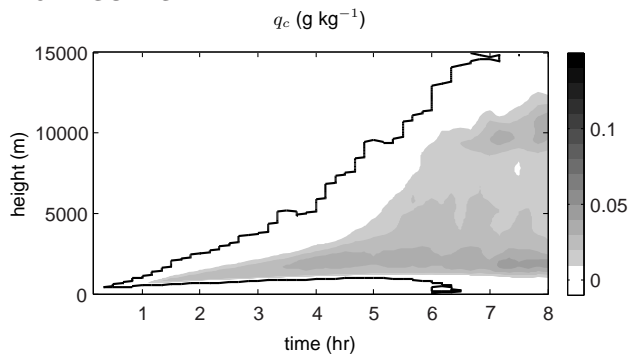


FIG. 1: Horizontal mean cloud condensate, reference case

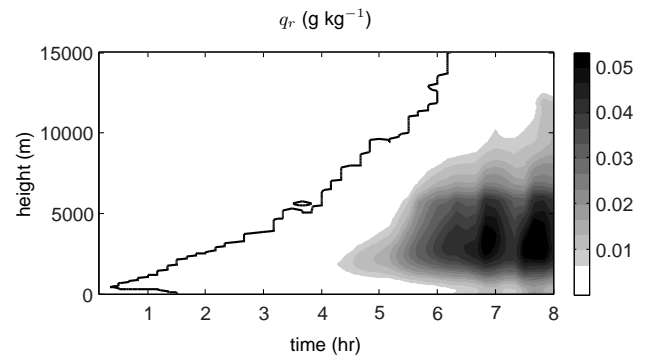


FIG. 2: Horizontal mean precipitation, reference case

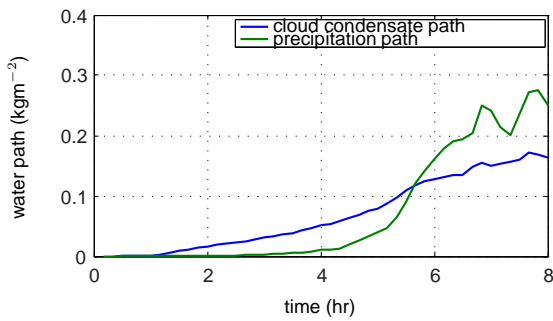


FIG. 3: Cloud condensate and precipitation path, reference case

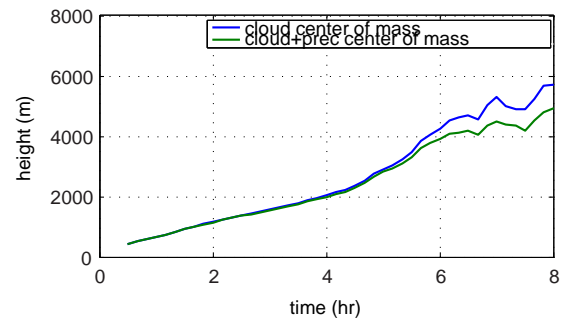


FIG. 4: Cloud center of mass, reference case

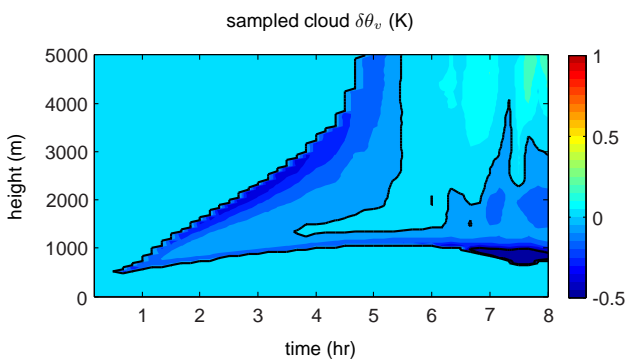


FIG. 5: Conditionally sampled buoyancy of clouds, reference case

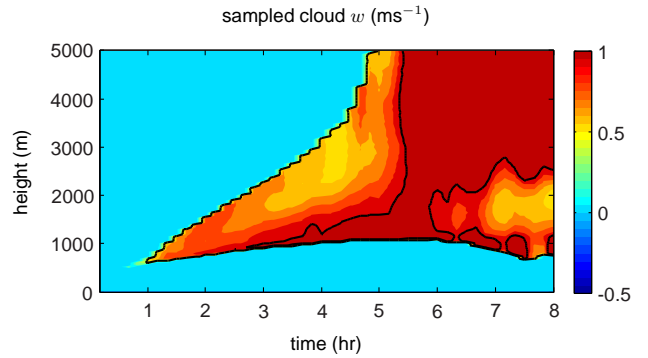


FIG. 6: Conditionally sampled vertical velocity of clouds, reference case, values are clipped at 1 ms^{-1}

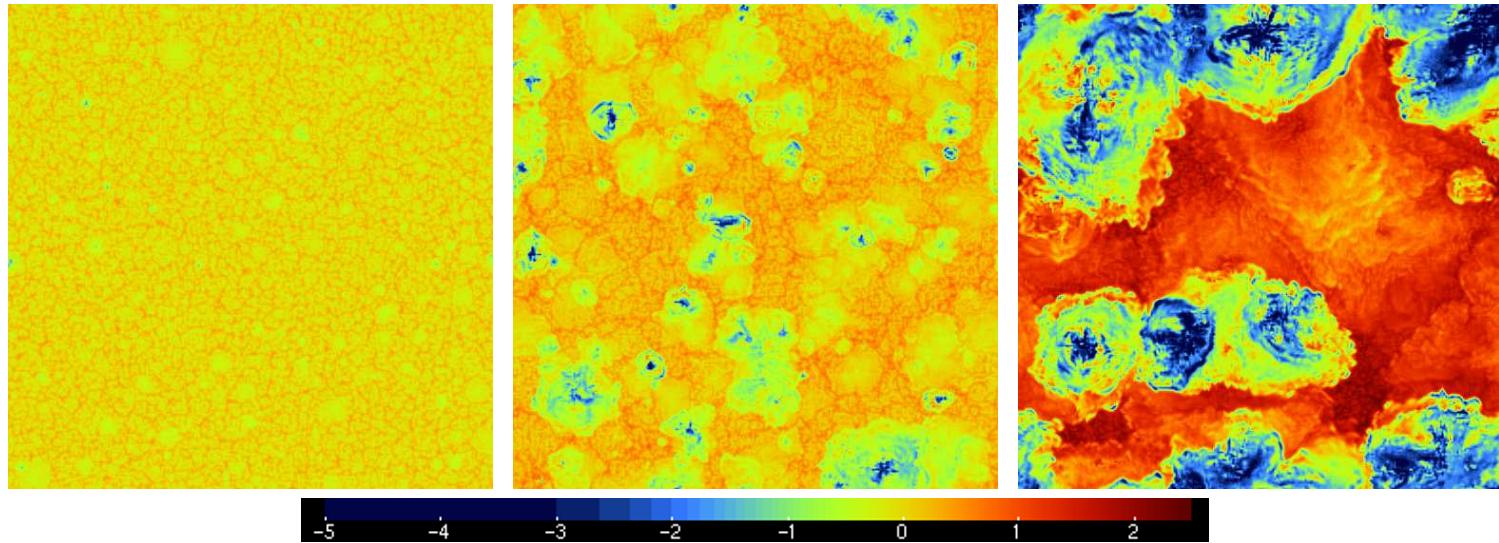


FIG. 7: Horizontal buoyancy field, $\theta_v - \overline{\theta}_v$ (K), at 100 meters after (left) 3, (middle) 5 and (right) 7 hours, reference case.

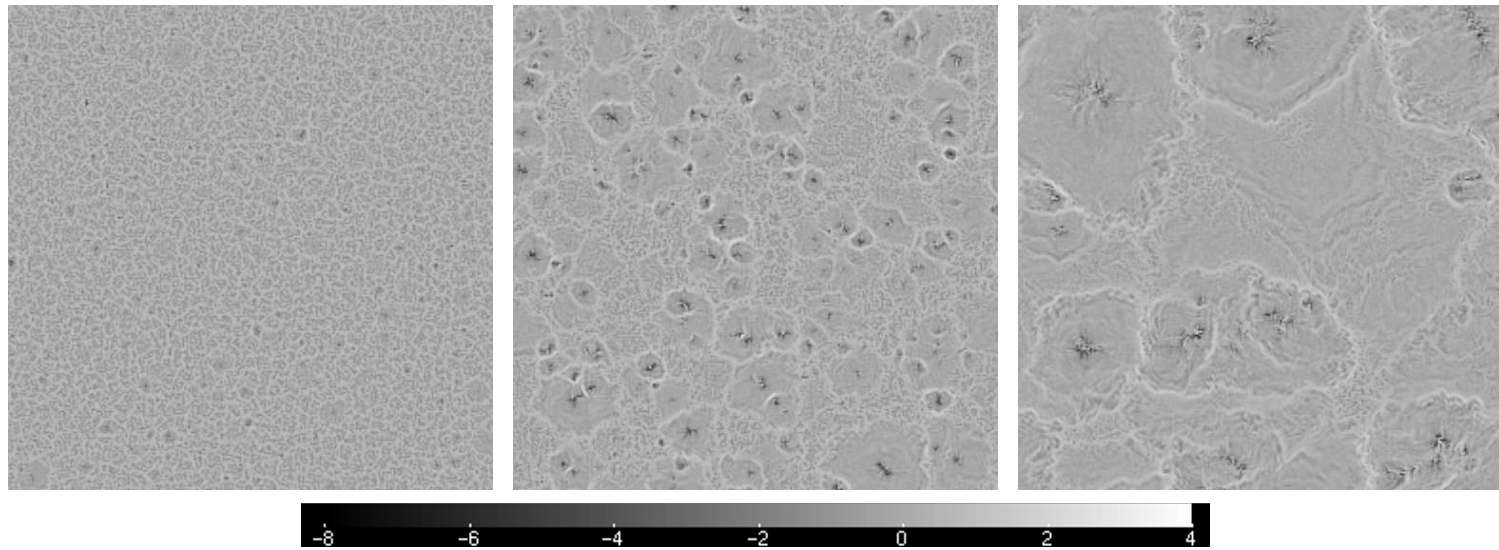


FIG. 8: Horizontal slice of vertical velocity field at 100 meters after (left) 3, (middle) 5 and (right) 7 hours, reference case. Strong downdrafts occur at the center of cold pools, whereas updrafts occur over a small distance at the edges.

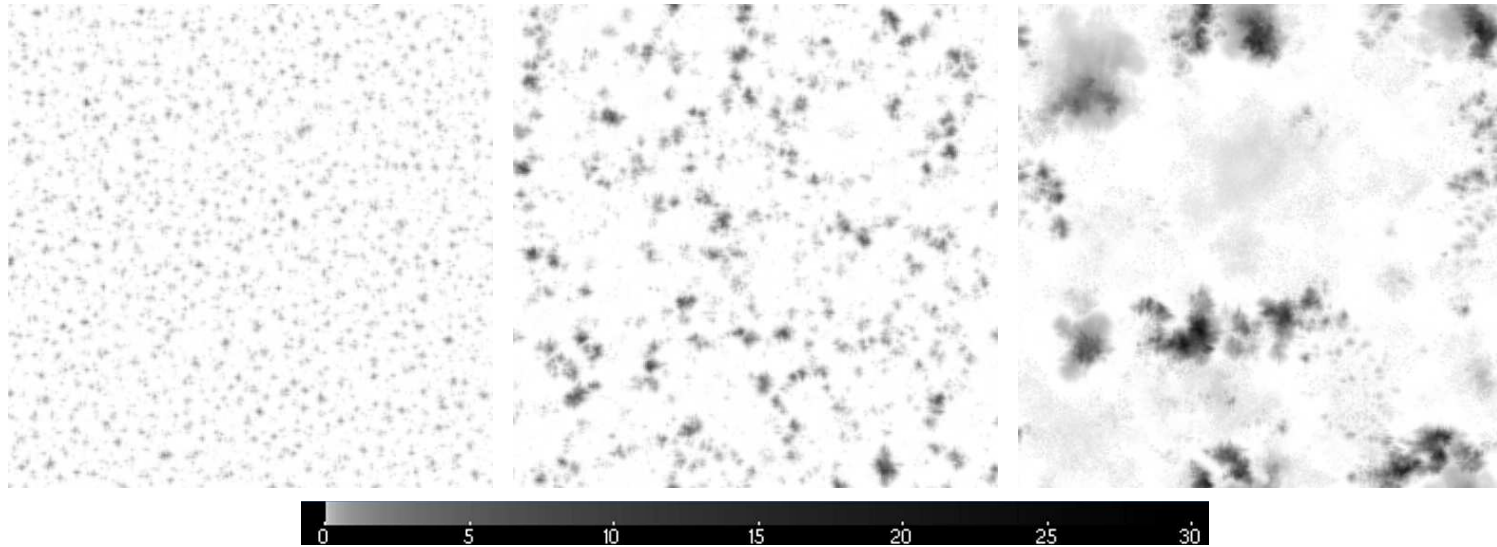


FIG. 9: Horizontal rain water path field at 100 meters after (left) 3, (middle) 5 and (right) 7 hours, reference case. Color shading is not linear for the purpose of visibility of rain water after 3 and 5 hours. Strong rainfall occurs at the center of cold pools.

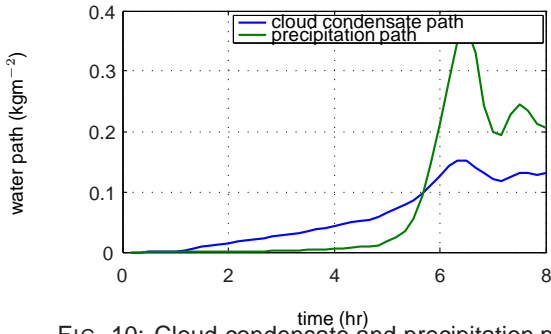


FIG. 10: Cloud condensate and precipitation path, filtering applied to the subcloud layer

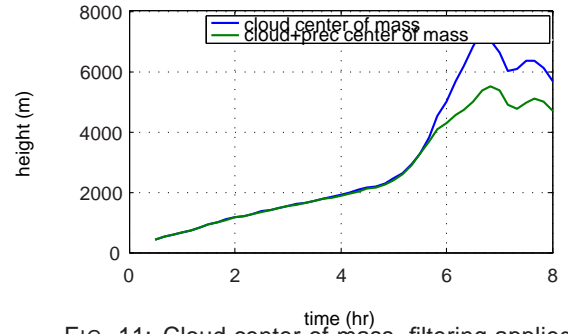


FIG. 11: Cloud center of mass, filtering applied to the subcloud layer

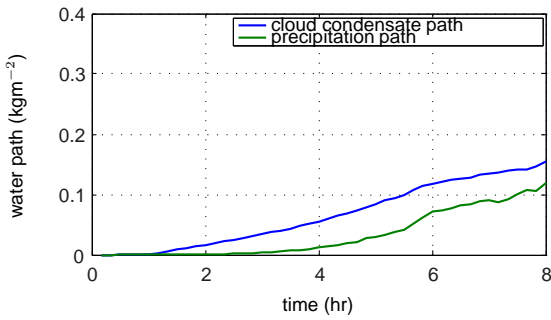


FIG. 12: Cloud condensate and precipitation path, horizontal mean evaporation applied to q_t and θ_t

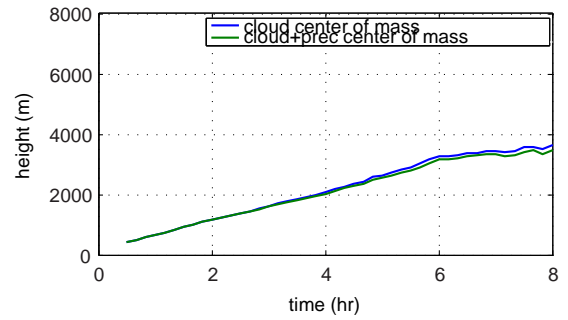


FIG. 13: Cloud center of mass, horizontal mean evaporation applied to q_t and θ_t

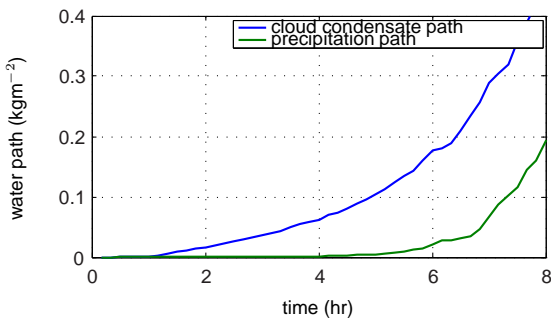


FIG. 14: Cloud condensate and precipitation path, without accretion

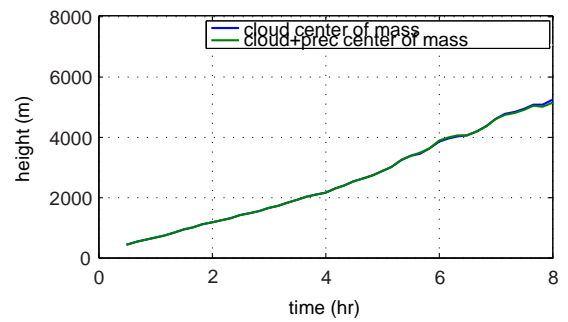


FIG. 15: Cloud center of mass, without accretion

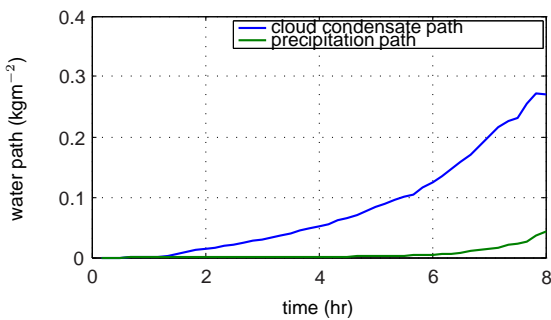


FIG. 16: Cloud condensate and precipitation path, without accretion and filtered

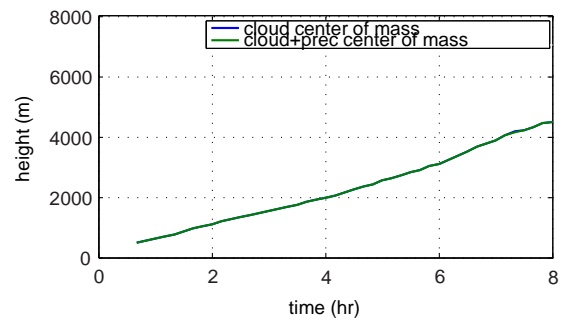


FIG. 17: Cloud center of mass, without accretion and filtered

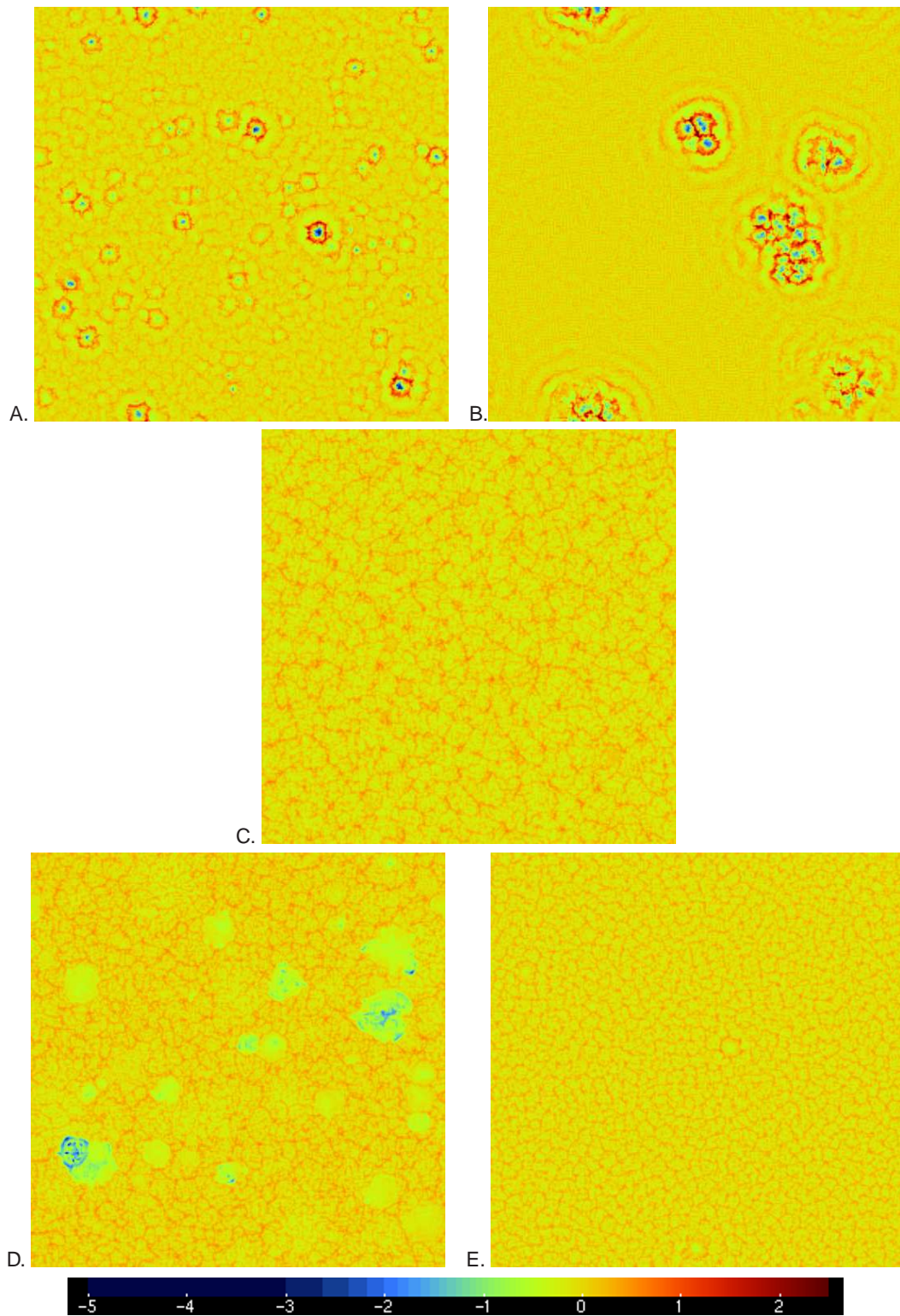


FIG. 18: Horizontal subcloud layer buoyancy field at 100 meters in simulations with altered subcloud dynamics and/or microphysics. A) Filtering the subcloud thermodynamics fields, after 5 hours B) Idem, after 7 hours C) Horizontal mean evaporation working on the thermodynamic fields, after 7 hours D) Without accretion, after 7 hours E) Idem, but with the filtering procedure

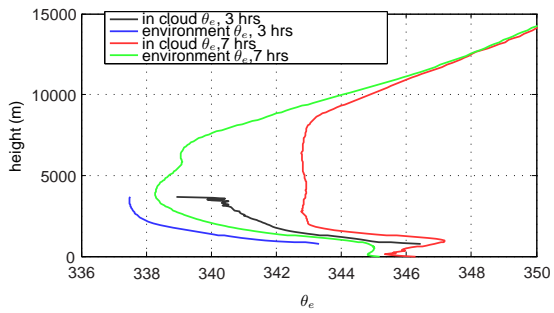


FIG. 19: Conditionally sampled θ_e , reference case.

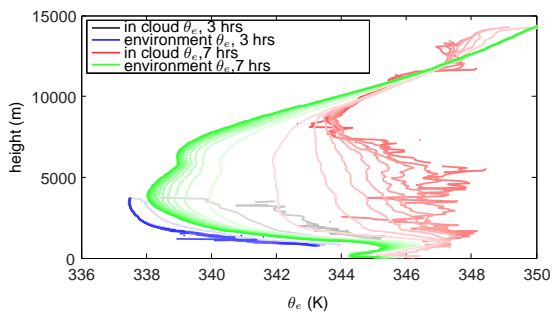


FIG. 20: Conditionally sampled θ_e , reference case. Color intensity reflects distance from cloud edge (in steps of 200 meters). A large difference between the dark colored core of the cloud and the environment is clear

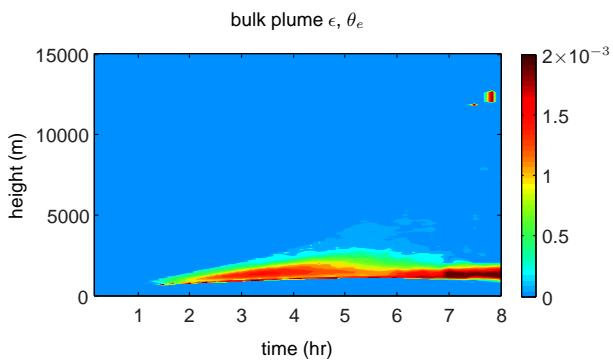


FIG. 21: Bulk plume fractional entrainment as estimated from θ_e , reference case